Techniques of Production and Analysis of Polarized Synchrotron Radiation

Dennis M. Mills
Advanced Photon Source
Argonne National Laboratory
9700 S. Cass Ave, Argonne, IL 60439

ABSTRACT

The use of the unique polarization properties of synchrotron radiation in the hard x-ray spectral region (E>3 KeV) is becoming increasingly important to many synchrotron radiation researchers. The radiation emitted from bending magnets and conventional (planar) insertion devices (IDs) is highly linearly polarized in the plane of the particle's orbit. Elliptically polarized x-rays can also be obtained by going off-axis on a bending magnet source, albeit with considerable loss of flux. The polarization properties of synchrotron radiation can be further tailored to the researcher's specific needs through the use of specialized insertion devices such as helical and crossed undulators and asymmetrical wigglers. Even with the possibility of producing a specific polarization, there is still the need to develop x-ray optical components which can manipulate the polarization for both analysis and further modification of the polarization state. A survey of techniques for producing and analyzing both linear and circular polarized x-rays will be presented with emphasis on those techniques which rely on single crystal optical components.

1. INTRODUCTION

The polarization of the radiation emitted from high energy accelerators has been of interest to experimenters for over three decades. This interest has evolved from the first measurements of the polarization of synchrotron radiation by Joos [1], who confirmed the theoretically predicted polarization dependence of radiation from the Cornell 1.1 GeV electron synchrotron, to present day researchers who are using the circularly polarized x-rays emitted out of the orbital plane from dedicated storage ring sources to investigate the magnetic properties of materials. In fact, the interest in polarization effects at x-ray wavelengths has grown to the point where specialized insertion devices are now being constructed to produce radiation with specific and/or tunable polarization states. (See article by K. J. Kim, these proceedings.) Even though the interest in the use of polarized x-rays is on the rise, progress in this area has been slow to develop due in large part to the difficulty in efficiently producing, manipulating, and analyzing beams of polarized x-rays. A variety of types of polarimeters have been used to measure the degree of linear polarization of synchrotron radiation beams at hard x-ray energies. However, the measure

of the degree of linear polarization of an electromagnetic radiation beam does not constitute a complete description of the polarization state for that beam. In the visible region of the spectrum, a complete polarization analysis is routinely accomplished by means of linear polarizers and a quarter wave plate [2]. Unfortunately, the extension of visible light optical components to the x-ray regime is not straightforward. Polarizing devices, such as linear polarizers and phase plates, are not prevalent for radiation in the x-ray region of the electromagnetic spectrum because dichroic and anisotropic effects are generally extremely weak at these frequencies. (Even near x-ray absorption edges, where resonant effects can come into play, the x-ray susceptibility anisotropies are still meager at best.) However, birefringence, dichroism, and polarization rotation is observed at or near Bragg reflections in crystals [3]. These diffractive effects can be considerably stronger than standard anisotropic effects, and diffraction-based devices for polarization manipulation and analysis look very promising. Although this paper will deal primarily with polarization phenomena using hard x-rays (E≥3 keV), some of the polarization phenomena observed in crystals with hard x-rays can also be observed with soft x-rays using multilayers.

2. COMPTON POLARIMETERS

2.1 Linear polarization analysis

One of the important predictions of the electromagnetic theory of radiation is that a ray scattered through an angle of 90° will become linearly polarized. Using this principle, C.G. Barkla in 1906 [4] verified the electromagnetic character of x-rays. Compton polarimeters [5], which also rely on this principle (see Fig. 1), have been used at several synchrotron radiation facilities to measure P_l, the degree of linear polarization. P_l is defined as:

$$P_l = (I_\sigma - I_\pi) / (I_\sigma + I_\pi) \qquad (1)$$

where I_σ (I_π) is the intensity of the σ (π) polarization component of the beam. (Throughout this text we will define π polarization as that component of the beam whose electric field vector lies in the plane of diffraction as defined the the incident and scattered wavevectors, and the σ polarization as that component whose electric field vector is perpendicular to the scattering plane.) Compton polarimeters have the advantage that they operate over wide energy ranges but are typically very inefficient since the Compton scatterer must be rather thin so that multiple scattering, which can degrade the resolving power of the polarimeter, is minimized. The fact that the Compton scatterer is thin and therefore attenuates only a small fraction of the total beam makes these devices ideal for monitoring strong incident beams such as those encountered at synchrotron radiation sources.

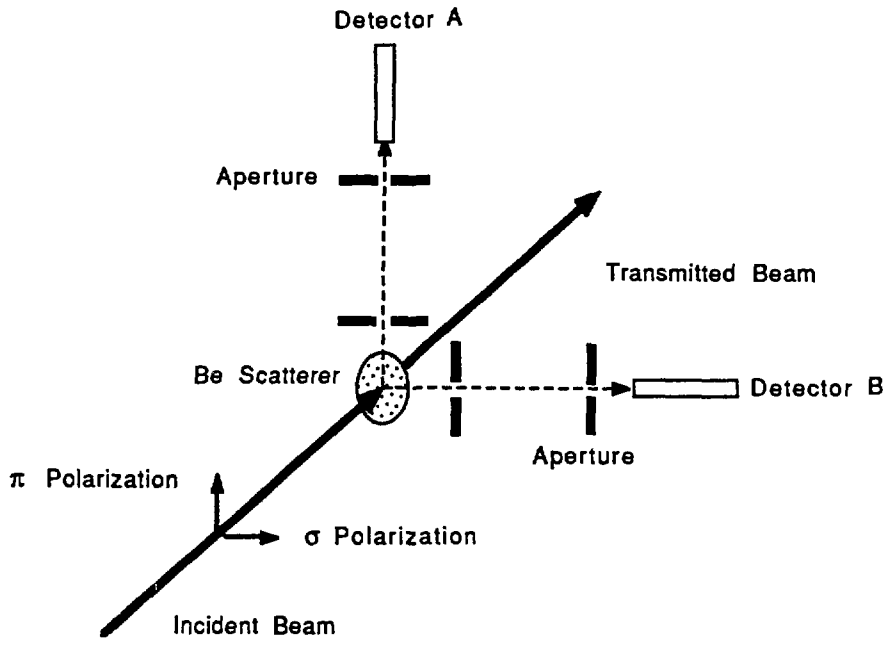

FIG. 1. Schematic of a Compton polarimeter for linear polarization analysis. The incoming beam, scattered by thin foil of Be, is detected by two detectors oriented at right angles to each other and to the beam. Apertures define the angular acceptance of the detectors. Detector A is sensitive to σ polarized x-rays while Detector B is sensitive to π polarized x-rays.

2.2 Circular polarization analysis

The use of Compton scattering for linear polarization analysis assumes the scattering process occurs through the interaction of the electromagnetic wave with the charge of the electron. This is certainly the dominant interaction. However, the electromagnetic wave can also interact with the spin and orbital momentum of the electrons [6] and interacts most strongly with that component of the beam which is circularly polarized. If the degree of circular polarization is defined as:

$$Pc = (I_r - I_l) / (I_r + I_l) \qquad (2)$$

where I_r and I_l are the intensities of the right and left circular polarizations respectively, then the leading terms in the cross-section for Compton scattering for a single electron can be written as [7]:

$$d\sigma/d\Omega = 1/2\, r_o^2\, (k_s/k_o)^2 \{\Phi_o + P_l\Phi_l + P_c\Phi_c(\varpi)\} \qquad (3)$$

where r_o is the classical electron radius, k_s (k_o) the scattered (incident) beam wavevector, P_l and P_c the

degree of linear and circular polarization respectively, Φ_0 ,Φ_1 and $\Phi_c(\sigma)$ the polarization independent, linear polarization dependent and circular polarization dependent Compton cross-sections respectively and σ the spin of the electron. Note that only the circular polarization cross-section is a function of σ; the first two terms are only dependent upon the scattering from the charge of the electron. By reversing the direction of the magnetization in the sample and making a difference measurement the magnetic term, which is proportional to the degree of circular polarization, can be isolated and P_c determined. This technique is particularly useful at higher x-ray energies because the magnetic cross-section scales as the photon energy and has been frequently used to determine the degree of circular polarization of gamma rays emitted from radioactive sources. Nonetheless, this technique can be used with lower energy x-rays as a powerful tool for the determination of P_c.

3. POWDER AND MOSAIC CRYSTAL POLARIMETERS

3.1 Linear polarization analysis

Bragg scattering from powders, perfect, and imperfect or mosaic crystals exhibits a suppression of the π component of the scattered beam whenever twice the Bragg angle ($2\Theta_B$) equals 90°. Bragg scattering polarimeters provide considerably higher efficiency than Compton polarimeters, but have one strong constraint. Whereas Compton scattering occurs with any incident photon energy, in Bragg scattering the incident wavelength must satisfy Bragg's Law for the polarizing crystal, i.e. $\lambda=2d\sin(45°)$, where d is the atomic planer spacing for the analyzer reflection being used. Depending on the divergence of the beam to be analyzed, powders and imperfect crystals may be advantageous over perfect crystals since the angular range of diffraction for powders and mosaic crystals can be considerably larger (fractions of a degree) than that for perfect crystals (arc seconds).

4. PERFECT CRYSTAL POLARIMETERS

The use of perfect single crystals can provide several solutions to the problem of analysis and production of polarized x-ray beams. Diffraction from perfect crystals in both the Laue (transmission) and Bragg (reflection) geometries can be used as linear polarizers and x-ray phase plates. To better understand how these polarizers work, it is necessary to review dynamical diffraction, the theory that describes x-ray diffraction in perfect crystals. (Several comprehensive reviews have been written [9,10], and the reader is referred to these for more details on x-ray dynamical diffraction.) Kinematic diffraction theory treats the scattering from each scattering volume element independently, while dynamical diffraction takes into account all wave fields within the crystal. This type of theory is essential when the intensity of the diffracted beam is of comparable strength to the incident x-ray beam, as is often the case in strong reflections from perfect crystals. Three important results of dynamical diffraction need to be highlighted in

order to understand most of the polarization properties of diffraction in perfect single crystals.

The first result of dynamical diffraction is that as the condition for Bragg diffraction in perfect crystals is approached, the incident and diffracted traveling waves interact and produce a standing wavefield within the crystal. If the crystal structure is simple enough, the period of these standing waves is exactly equal to the interatomic spacing of the diffracting planes. In the Bragg geometry there is only one standing wave (for each polarization), but in the Laue geometry there are two standing wavefields (for each polarization), each 180° out of phase with the other. One set of wavefields has it nodes located on the atomic planes (the so-called α wavefields) while the other set (β wavefields) has its nodes located between the atomic planes (See Fig. 2). If we make the simple assumption that the overlap of the wavefield and the charge density is a measure of the interaction between the x-rays and the crystal, then we see that the α wavefields interact with the crystal much less than an x-ray wavefield at an arbitrary orientation in the

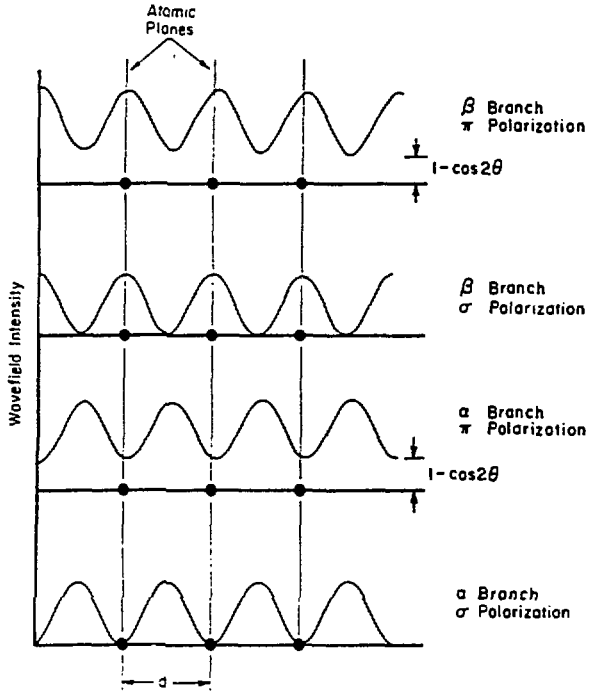

FIG. 2. Standing wavefields that occur in the crystal as a consequence of the overlap of the incident and Bragg scattered waves. The standing waves labeled β have their anti-nodes at the atomic planes and interact much more strongly with the crystal than the standing waves labeled α, which have their nodes at the atomic planes. Notice that the s polarized standing wavefields go to zero at their minima but the π polarized component for both the α and β wavefields exhibit incomplete cancellation and the minima of the wavefield does not go to zero. This fact results in a slightly different interaction for each of the four standing wavefields in the crystal.

crystal, while the β wavefields have a greater interaction with the crystal than an arbitrarily oriented wavefield. Put in a more qualitative way, when the crystal is isotropic, all wavefields in the crystal have the same wavevector given by (following the notation of Hart [3]):

$$|\mathbf{K}| = k\,(1 + 1/2\,\chi_0) \qquad (4)$$

where k is the vacuum wavevector and χ_0 is the zero order Fourier coefficient of the electric susceptibility which is given by:

$$\chi_h = -(r_o \lambda^2 F_h)/(\pi a_o^3) \qquad (5)$$

where λ is the x-ray wavelength, F_h the structure factor, and a_o^3 the volume of the unit cell. However, at the Bragg condition:

$$|K| \neq |K_\alpha| \neq |K_\beta| \qquad (6a)$$

and

$$\mu \neq \mu_\alpha \neq \mu_\beta \qquad (6b)$$

where K (μ) is the wavevector (absorption coefficient) for a randomly oriented wavefield, and $\mathbf{K}_i$ (μ_i) is the wavevector (absorption coefficient) associated with the i^{th} wavefield. When the difference between the two polarizations are included, the crystal can exhibit four-refringence and dichroic properties, i.e.;

$$|K| \neq |K^\sigma_\alpha| > |K^\pi_\alpha| > |K^\pi_\beta| > |K^\sigma_\beta| \qquad (7a)$$

and

$$\mu \neq \mu^\sigma_\alpha < \mu^\pi_\alpha < \mu^\pi_\beta < \mu^\sigma_\beta \qquad (7b).$$

The second pertinent result of dynamical diffraction is that even in a perfect crystal of infinite extent, there is a finite angular range of near perfect reflectivity for a crystal in the Bragg geometry. This angular range, often called the Darwin width, is well defined and given by:

$$\omega_D = |\chi_h| |P| / \sin(2\Theta_B) \qquad (8)$$

where Θ_B is the Bragg angle, and P, the polarization factor, which equals 1 or $\cos(2\Theta_B)$ for σ and π polarizations respectively. One might expect the range of the diffraction to be vanishingly small since, on physical grounds, the diffraction from an infinite set of perfectly aligned planes would result in a peak whose width would approach zero. (Mathematically speaking, the Fourier transform of a perfectly periodic structure of infinite extent would be a series of delta-functions.) The origin of this finite width arises from the fact that the x-rays do not see an infinite crystal but are scattered out after a characteristic length, L_e, called the extinct length. (This is a distinctly different quantity than the absorption length, L_a, which determines the extent of propagation in a material due to absorption processes. For strong reflections in perfect crystals $L_e << L_a$. See references [8] for more detail.) There is also a polarization

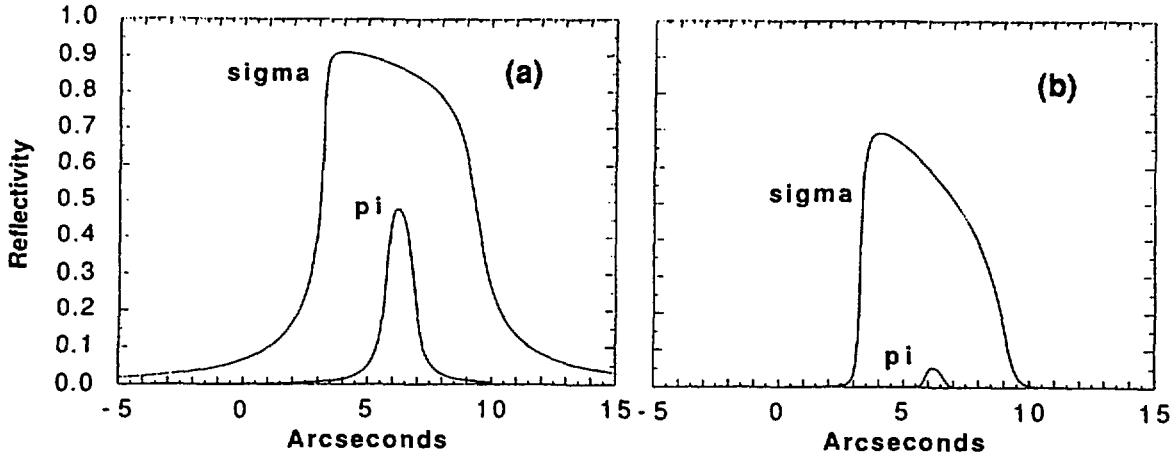

FIG. 3. (a) Reflectivity curves for σ and π components for one reflection from Ge (440) planes at 1.54 Å. Notice that the width and height of the reflectivity curve for the π polarized component is considerably less than the σ component. (b) Reflectivity curves after four Bragg reflections from the Ge (440) planes. The ratio of the areas under the σ and π curves in (b) is about 100 to 1. Even better rejection ratios can be achieved by introducing a small angular offset, on the order of the Darwin width, between the crystals.

dependence on the Darwin width (See Fig. 3); the breadth of the Darwin curve associated with the π polarized wave is smaller than that associated with the σ polarized wave by the factor $\cos(2\Theta_B)$, a consequence of the decreased scattering cross-section for π polarized radiation.

The third important result of dynamical diffraction is that in the Bragg geometry, as the crystal is rotated through the Darwin width, the phase of the diffracted wave changes by 180°. In terms of the standing waves described earlier, the standing waves cross from the α type wavefields to the β type wavefields as the crystal is rotated through this region of near total reflection. The crossing from the α to the β wavefields manifests itself through the asymmetric shape of the Darwin curve; the higher reflectivity side corresponds to the α wavefields which have a smaller effective absorption coefficient while the lower reflectivity side correspond to the β wavefields which have a higher effective absorption coefficient (See equation 6b). It is these three features of the theory of dynamical diffraction that account for most of the effects described below.

4.1 Linear polarizers

The use of diffractive dichroism in perfect crystals for linear polarizers was first proposed in 1961

by Cole, Chambers, and Wood [9]. Using the anomalous transmission or Borrmann effect [10] in perfect crystals, one state of the polarization can be preferentially absorbed. This is accomplished by selecting the thickness of the Laue crystal such that the only remaining wavefield which exits the crystal is the σ polarized components from the α wavefields. Although effective, Borrmann polarizers have several drawbacks including low efficiency and, for a given x-ray energy, a narrow angular acceptance, typically several arc seconds.

One way to overcome some of the drawbacks of the Borrmann polarizer is to use multiple Bragg reflections as a means of suppressing one of the polarization states. By utilizing the difference in angular width of the Darwin curves between σ and π polarized x-rays (see Fig. 3), the π component of the radiation can be preferentially removed relative to the σ component. Because the reflectivity at the Bragg condition is nearly unity for σ polarized x-rays, multiple reflections can be used to enhance the rejection of the π polarized x-rays with little intensity loss to the σ polarized x-rays. Hart and Rodrigues [11] have shown that one can not only enhance the rejection of the π polarization, but that these multiple bounce reflections can also be used over a wide range of wavelengths with rejection ratios of 10^{-4} or greater. The wavelength range over which these multiple bounce linear polarizers can operate can be increased if an angular offset is made between the crystals. Typically this offset is enough eliminate the overlap of the π polarized reflectivity curve, but not enough to eliminate overlap of the σ polarized reflectivity curve. Using this technique, an x-ray beam in the wavelength range from 1 to 3 Å can be linearly polarized to better than one part in 10^{-5} with a complement of six different four-reflection polarimeters [11].

3.2 Circular polarizers

The development of circular polarizers or x-ray phase plates has been much slower than that of linear polarizers. However, over the last several years there has been renewed interest in the development of x-ray phase plates, driven in part by the interesting developments that have recently occurred in the field of magnetic x-ray physics. (This includes magnetic elastic or Bragg scattering studies, magnetic inelastic or Compton scattering studies, and magnetic x-ray absorption studies.) In addition, the availability of high flux, well collimated, and (relatively) highly polarized x-ray beams emitted from synchrotron radiation sources have become more readily available. These beam properties are often precisely what is needed in order to make x-ray phase plates operate effectively and efficiently.

The diffractive birefringence of perfect crystals at the Bragg condition (in the Laue geometry) has been proposed theoretically and shown experimentally to produce circular polarized x-rays by several groups [12]. An x-ray phase plate was first used at a synchrotron by Golovchenko et al. [13], and

extensions of that original work have been made by Mills [14]. The basic principles of operation of an x-ray phase plate are the same as those of a optical phase plate. The phase plate is oriented relative to a linearly polarized incident beam so that the incident beam is split into two orthogonally polarized coherent beams; the π and σ diffracted beams. In the Laue geometry, four diffracted wavefields are generated given by the four wavevectors in the right hand side of Equation (7a). Because the α and β wavefields are 180° out of phase, when they exit the crystal the wavefields recombine to produce linear polarized x-rays. The obvious solution to this problem is to eliminate one set of wavefields. This can be readily accomplished due to the differences in effective absorption coefficients between the α and β wavefields. The final thickness for the phase plate is then determined by adequate absorption of the β wavefields (relative to the α fields) and an accumulated phase shift of an odd multiple of 90° between the π and σ waves of the α fields. Depending on the phase plate material and x-ray wavelength at which it is to be used, a 3/4 or 5/4 phase shift may be required in order to adequately eliminate the β wavefields so that a high degree of circular polarization can be attained. The phase shift, ϕ, between the π and σ components of the α

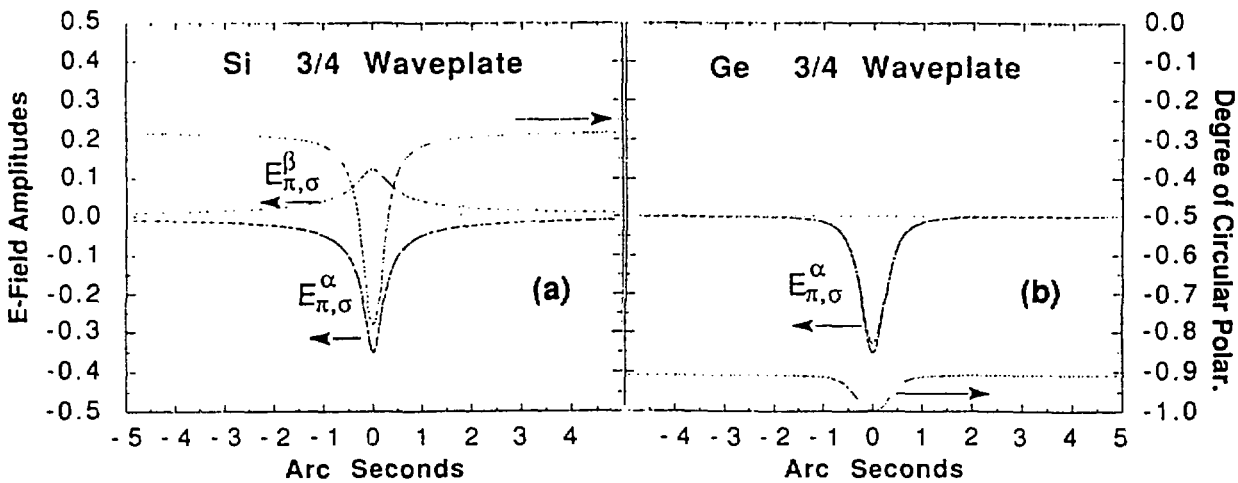

FIG. 4. The electric field amplitudes and degree of circular polarization as a function of angle for (a) a Si 3/4 waveplate (b) and a Ge 3/4 waveplate. Both calculations were made using the (400) reflections at 50 KeV. In the Si case, even exactly at the Bragg condition (0 arc seconds) the degree of circular polarization is not -1 ($\pm$1 signifies totally right hand/left hand circularly polarized). This is due to the fact that the β wavefields have not been attenuated sufficiently and combine with the α wavefields to produce linearly polarized radiation. In the Ge crystal however, the β wavefields have been completely attenuated (due to the larger absorption coefficient of Ge as compared with Si) and the resultant diffracted beam has a much higher degree of circular polarization. Here the degree of circular polarization at a particular angle, δ, is the total polarization for an incident beam with divergence $\pm\,\delta$.

is given by:

$$\phi = 2\pi(K^{\sigma}_{\alpha} - K^{\pi}_{\alpha}) \cdot R \qquad (9)$$

For a symmetrically cut crystal at the exact Bragg condition, i.e. $\Delta\Theta = 0$, this can be written as:

$$\phi = (\pi t_o \chi_h / \lambda \cos(\Theta_B))\{1 - |\cos(2\Theta_B)|\} \qquad (10)$$

where t_o is the thickness of the crystal. In general, the phase shift experienced is a function of $\Delta\Theta$, the deviation from the Bragg angle, and so for a divergent incident beam the net polarization will be considerably less than that of the central ray ($\Delta\Theta = 0$). Figure 4 shows the calculated electric field amplitudes and degree of circular polarization for a silicon and germanium 3/4 phaseplate at 50 KeV. At high x-ray energies, a considerable improvement in the degree of circular polarization can be achieved with a germanium phase plates as compared with silicon due to the increased β wavefield absorption associated with germanium. At lower photon energies (E<20 KeV), the optimal crystal thicknesses are less than a millimeter and the phase plates become more difficult to fabricate. Fortunately, at these lower energies,

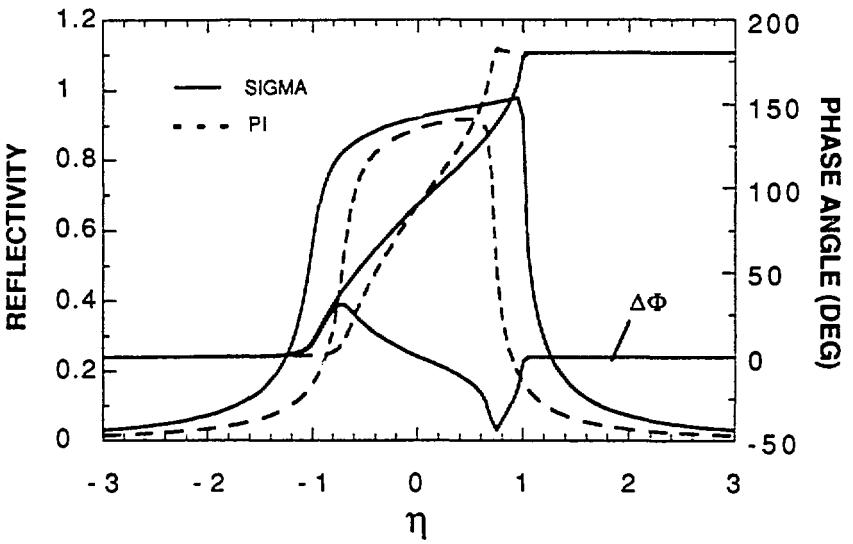

FIG. 5. Reflectivity, phase angle, and phase angle difference as a function of η (the scaled angle variable) for the σ and π components of the (220) reflection in Ge at 8 KeV. Because the phase difference is less that 90° per reflection multiple reflections are required to accumulate a total phase shift of 90° between the σ and π components. (With permission from B.W. Batterman, to be published).

Bragg reflection phase plates look to be a very attractive alternative. Phase plates operating in the Bragg geometry rely on the difference in the Darwin widths for σ and π polarized x-rays [15]. As mentioned earlier, the phase of the diffracted wave changes by 180° as one goes through the reflectivity curve. Hence at a given angle in the reflection curve, the σ and π components will have undergone differing phase changes (See Figure 5). The difference in phase between the two polarization components does not reach a full 90° which would be required for the transformation of linear polarized x-rays to circular polarized x-rays. Repeated reflections can cause a net accumulated phase difference of 90° producing a output beam that should be highly circularly polarized. As in the Laue geometry phase plate the accumulated phase shift is a function of $\Delta\Theta$ and therefore this device will operate best with a highly collimated incident beam. The relative phase shift difference for the σ and π polarizations described above for perfect crystals also occurs in layered synthetic microstructures (LSMs). LSMs have periods typically one to two orders of magnitude larger than crystals, and therefore may be useful as reflection phase plates for ultra-violet and very soft x-rays [16].

5. SUMMARY

Interest in x-ray polarimetry has grown substantially within the synchrotron radiation research community over the last several years This has been in large part motivated by recently developed experimental techniques which require accurate determination of the polarization state of the incident and scattered beams and the enhanced efficiency of polarizing components that the unique properties of synchrotron radiation has afforded. The new, high brilliance insertion device based x-ray synchrotron radiation sources being constructed, such as the Advanced Photon Source at Argonne National Laboratory, the European Synchrotron Radiation Source at Grenoble, France and the Super Photon Ring facility at Nashi Harima, Japan, will foster increased work in fields such as magnetic x-ray scattering [17], nuclear coherent scattering [18] and x-ray optical activity [19] which show extremely interesting x-ray polarization phenomena and open currently unforeseen avenues of research, many of which could require polarization analysis of the incident and scattered beams. In addition, these new sources will also permit novel and innovative insertion devices to be installed which have been designed specifically to produce radiation of a particular polarization state. Polarization analysis of the output beams will become an integral part of the characterization of these new insertion devices. All these efforts will require continued work on more efficient and more effective linear and circular polarizers for radiation at x-ray wavelengths.

5. ACKNOWLEDGEMENTS

This work supported by the U.S. Department of Energy, BES-Materials Science under contract no. W-31-109-ENG-38. The author would also like to thank B.W. Batterman for the use of the unpublished plot of Figure 5.

6. REFERENCES

1. Joos, P., Phys. Rev. Letts.,**4**, p558, 1960.
2. Klein, M. V. and Furtak, T. E., *Optics*, 2nd Ed., p623, John Wiley & Sons, Inc., 1986
3. Several excellent review articles on x-ray polarization phenomena have been written including, Skalicky, P. and Malgrange, C., Acta Cryst. A28, p501, 1972, Hart, M., Phil. Mag. B, **38**, p41, 1978, and Belyakov, V. A. and Dmitrienko, V.E., Sov. Phys. Usp., **32**, p697, 1989.
4. Barkla, C. G., Proc. R. Soc., **77**, p247, 1906.
5. Hannon, J.P. and Trammel, G.T., Phys. Rev., **186**, p306, 1969.
6. Platzman P.M. and Tsoar, N., Phys. Rev. B, **2**, p 3556, 1970.
7. Mills, D. M., Phys. Rev. B, **36**, p6178, 1987.
8. Batterman, B. W. and Cole, H., Rev. Mod. Sci., **36**, p681, 1964 and James, R.W., Solid State Physics, **13**, p53, 1963.
9. Cole, H., Chambers, F. W. and Wood, C. G., Jour. of Appl. Phys., **32**, p1942, 1961.
10. Borrmann, G., Z. Krist., **106**, p109, 1954 and **112**, p312, 1959.
11. Hart, M. and Rodrigues, A.R.D., Phil. Mag. B, **40**, p149, 1979.
12. Brummer, O., Eisenschmidt, C., and Hoche, H.R., Crys. Res. and Tech., **18**, p241, 1983; and Hart in ref. [4].
13. Golovchenko, J.A., Kincaid, B. M., Levesque, R.A., Meixner, A.E. and Kaplan, D. R., Phys. Rev. Letts., **57**, p202, 1986.
14. Mills, D. M., Nuc. Inst. and Meths., **A266**, p531, 1988. Note there are two corrections to this paper; Eqn. (3) should read $y = [(\Delta\Theta)\sin(2\Theta)\pi V]/[r_e \lambda^2 |F_{\mathbf{H}}|]$, and Eqn. 4 should read $Z_{\pi,\sigma} = [(r_e \lambda |F_{\mathbf{H}}| |P|) / (2\pi V)][(y^2 + 1)^{1/2} - (y^2 + \cos(2\Theta))^{1/2}]$.
15. Batterman, B.W., Acta Cryst., **A40**, Supplement, 1984; and Brummer, O., Eisenshcmidt, C., and Hoche, R., Acta Cryst., **A40**, p394, 1984.
16. Kortright, J. B. and Underwood, J.H., to be published in the Proceedings of the Synchrotron Radiation Instrumentation 89 Conference, Berkeley, CA, August 7-10, 1989.
17. Blume, M. and Gibbs, Doon, Phys. Rev. B, **37**, p1779, 1988.
18. Siddons, D. P., Hastings, J.B., Faigel, G., Berman, L.E., Haustein, P.E. and Grover, J.R., Phys. Rev. Letts., **62**, p1384, 1989.
19. Siddons, D.P., Hart, M., Amemiya, Y., and Hastings, J.B., Phys. Rev. Letts., **64**, p1967, 1990.